Shock Wave and High Pressure Phenomena

For further volumes:
http://www.springer.com/series/1774

Shock Wave and High Pressure Phenomena

L.L. Altgilbers, M.D.J. Brown, I. Grishnaev, B.M. Novac, I.R. Smith, I. Tkach, and Y. Tkach : Magnetocumulative Generators

T. Antoun, D.R. Curran, G.I. Kanel, S.V. Razorenov, and A.V. Utkin : Spall Fracture

J. Asay and M. Shahinpoor (Eds.) : High-Pressure Shock Compression of Solids

S.S. Batsanov : Effects of Explosion on Materials: Modification and Synthesis Under High-Pressure Shock Compression

G. Ben-Dor : Shock Wave Reflection Phenomena

L.C. Chhabildas, L. Davison, and Y. Horie (Eds.) : High-Pressure Shock Compression of Solids VIII

L. Davison : Fundamentals of Shock Wave Propagation in Solids

L. Davison, Y. Horie, and T. Sekine (Eds.) : High-Pressure Shock Compression of Solids V

L. Davison and M. Shahinpoor (Eds.) : High-Pressure Shock Compression of Solids III

R.P. Drake : High-Energy-Density Physics

A.N. Dremin : Toward Detonation Theory

V.E. Fortov, L.V. Altshuler, R.F. Trunin, and A.I. Funtikov : High-Pressure Shock Compression of Solids VII

B.E. Gelfand, M.V. Silnikov, S.P. Medvedev, and S.V. Khomik : Thermo-Gas Dynamics of Hydrogen Combustion and Explosion

D. Grady : Fragmentation of Rings and Shells

Y. Horie, L. Davison, and N.N. Thadhani (Eds.) : High-Pressure Shock Compression of Solids VI

J.N. Johnson and R. Chere´t (Eds.) : Classic Papers in Shock Compression Science

V.K. Kedrinskii : Hydrodynamics of Explosion

C.E. Needham : Blast Waves

V.F. Nesterenko : Dynamics of Heterogeneous Materials

S.M. Peiris and G.J. Piermarini (Eds.) : Static Compression of Energetic Materials

M. Sućeska : Test Methods of Explosives

M.V. Zhernokletov and B.L. Glushak (Eds.) : Material Properties under Intensive Dynamic Loading

J.A. Zukas and W.P. Walters (Eds.) : Explosive Effects and Applications

Boris E. Gelfand • Mikhail V. Silnikov •
Sergey P. Medvedev • Sergey V. Khomik

Thermo-Gas Dynamics of Hydrogen Combustion and Explosion

With 330 Figures

Springer

Boris E. Gelfand
Sergey P. Medvedev
Sergey V. Khomik
N.N. Semenov Institute of Chemical Physics RAS
Moscow
Russia

Mikhail V. Silnikov
Special Materials Corp.
Saint Petersburg
Russia

ISBN 978-3-642-25351-5 e-ISBN 978-3-642-25352-2
DOI 10.1007/978-3-642-25352-2
Springer Heidelberg Dordrecht London New York

Library of Congress Control Number: 2012930644

Printed on acid-free paper

Springer is part of Springer Science+Business Media (www.springer.com)

Dedicated to the warm memory of Polenov A.N. and Popov O.E.,
our colleagues and friends untimely deceased.

Preface

The high potential heat production and high reactivity of hydrogen are unique properties that attract great attention of investigators. In the last 10 years, a hailstorm of various publications on this topic has been issued. Investigations of hydrogen explosion processes take a special place in the ranks of such articles and presentations. The dynamics of the increase in publications can be evaluated by comparing information generalized and systematized in [1] and [2]. The totality of data on specific subjects related to the details of hydrogen explosion phenomena can be found in [3–14].

The data base stored on this issue has been constantly increasing with new investigations and publications; the results, which are of great value for use in hydrogen storage operations and its safe industrial application, have being systematized. It is very important to get rid of groundless fears of using hydrogen as an energy carrier that are caused by lack of trustworthy data on the thermo-gas dynamic parameters of hydrogen combustion and explosion processes. Conditions, under which hydrogen is used, constrain the application of standard hydrocarbon utilization schemes; it is necessary to take into consideration the specifics in getting a solution to a particular problem.

However, application of new schemes does not create insuperable hindrances; usage of innovative technologies is grounded on a complete database of hydrogen as a new type of fuel. Founders of combustion theory called upon investigators to generalize and accumulate data considered from both scientific and practical points of view.

It is clear from the above dedication (Fig. 1) that even in 1985 Ya.B. Zeldovich was optimistic about renewal of combustion and detonation sciences. His optimism was based on the confidence that basic representations of explosion phenomena, given in classical works, would be developed and broadened by describing new combustible systems.

The validity of Ya.B. Zeldovich's prediction has been proven when problems of using hydrogen as a promising fuel for high-efficiency and ecologically clean technologies have arisen.

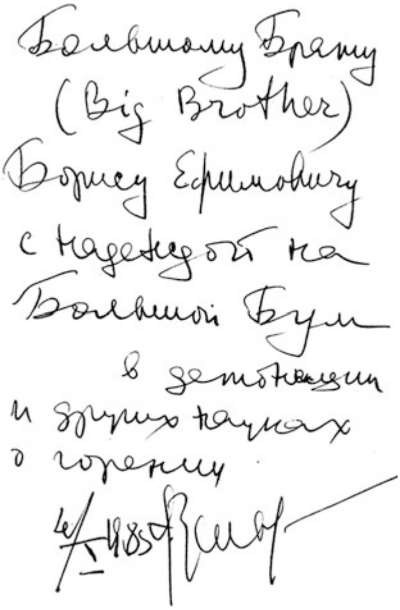

Большому Брату
(Big Brother)
Борису Ефимовичу
с надеждой на
Большой Бум
в детонации
и других науках
о горении
6/I 1985

Fig. 1 Dedication of Academician Ya.B. Zeldovich to B.E. Gelfand (To my Big Brother Boris with hope for a Big Boom in detonation and other combustion sciences)

Figure 2 and Tables 1, 2, and 3 represent the comparison diagram of ten parameters characterizing combustion and detonation of hydrogen and a typical current fuel (benzine). Hydrogen as a fuel is unique in relation to its detonability, its combustion limits, its flame velocity and extremely low ignition energy.

Due to the various subjective and objective reasons the book on hydrogen combustion and explosion published recently [2] does not include some useful data on combustion limits of binary fuels containing hydrogen. The class of binary fuels (for example, hydrogen+hydrocarbon) significantly widens options of potential safety use of hydrogen as a fuel.

The scheme of the data analysis presented in [2] broadens the concept of the current situation specified by problems of using known chemical reaction schemes while analyzing explosion phenomena which occur in practically important temperature and pressure ranges of combustible mixtures. The role of chemical reactions and gas dynamic processes is greatly divided for their model-surrogates where their feedback is assumed to be suppressed on the grounds of wrongfully and non-typically decreased energy paths.

Special attention has been paid to explosion phenomena accompanied by high pressure loads on structures. Such phenomena include reflections of detonation waves with extensive reaction zones near the detonation limits [3, 15–18] and collisions of non-stationary complex shock waves+combustion fronts with obstacles during DDT process.

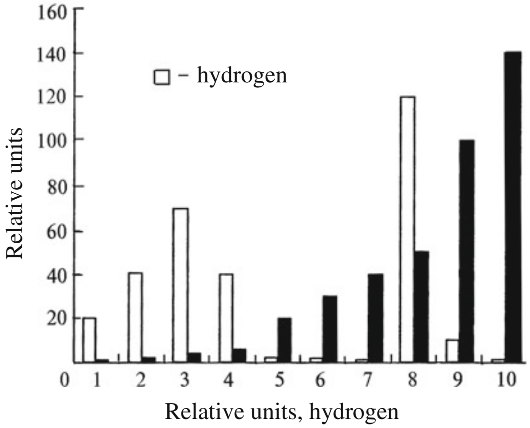

Fig. 2 Comparison diagram of hydrogen/benzine properties: *1* – buoyancy; *2* – detonability; *3* – combustion limits; *4* – flame velocity; *5* – fire hazard; *6* – molecular weight; *7* – flame radiation; *8* – energy per mass unit; *9* – energy per volume unit; *10* – ignition energy [5]

Table 1 Combustion process parameters

Parameter	Hydrogen	Methane	Benzine
Concentration limits of combustion	4–75 vol.% α=0.1–2.5	5–15 vol.% α=0.53–1.7	1.0–7.6 vol.% α=0.7–1.8
Stoichiometric composition in air, vol.%	29.53	9.48	1.76
Min ignition energy, mJ	≈0.02	≈0.29	≈0.24
Ignition temperature, K	≈750	≈810	≈500–770
Flame temperature, K	≈2,300	≈2,150	≈2,470
Normal flame velocity, cm/s	≈265–325	≈37–545	≈37–543
Max quenching gap, cm	≈0.064	≈0.203	≈0.2
Fraction of energy to radiation, %	≈17–25	≈23–32	≈30–42

Table 2 Fuel thermodynamic parameters

Parameter	Hydrogen	Methane	Benzine
Molecular weight	2.016	16,043	107
Gas density at normal conditions, g/m^3	83.76	651.19	4,400
Calorific efficiency, kJ/g	**119 (low)** **142 (high)**	**50 (low)** **55 (high)**	**44 (low)** **48 (high)**
Specific heats ratio	1.383	1.308	1.05
Diffusion coefficient, cm^2/s	0.61	0.16	0.005
Specific heat, J/g ·	14.89	2.22	1.62

Data on diffusion flame parameters of hydrogen jet discharges into the surroundings have been summarized as an additional dangerous factor used for the analysis of safe hydrogen transportation. Conditions of spontaneous ignition of both hydrogen and its mixtures with combustible and incombustible additives have been

Table 3 Parameters of aviation fuel/propellant

Parameter	Hydrogen	Methane	Kerosene
Composition	H_2	CH_4	$C_{12,5}H_{24,4}$
Boiling point T, °C	−252.7	−161	167–266
Density at T, g/cm^3	≈0.071	≈0.423	≈0.8
Calorific efficiency, kJ/kg	≈119,970	≈48,140	≈49,100
Flame temperature, K	≈2,300	≈2,150	≈2,400
Evaporation heat, J/g	≈440	≈510	≈360
Concentration limits of combustion, vol.%	4–75	5–15	0.84–6
Concentration limits of detonation, vol.%	13–65	6.3–13.5	1.1–3.3
Min Ignition energy, mJ	≈0.02	≈0.29	≈0.25
Min HE charge for detonation initiation, kg THT	≈0.00l	>10	≈1
Self-inflammation temperature in the air, K	≈750	≈810	≈600–700
Radiation energy, %	17–25%	23–32%	33–43
Toxicity	Not toxic	Not toxic	At > 500 ppm

specified. The authors hope that the present monograph can play a role as a guide in an ocean of data useful for specialists working with hydrogen as a fuel or a working medium in various technological processes.

References

1. B.E. Gelfand, S.B. Dorofeev, B.B. Chaivanov, F.V. Bezmelnitzin, Explosion characteristics of hydrogenous mixtures, Moscow. IRIS-91/5 (1991), 156 p.
2. B.E. Gelfand, O.E. Popov, B.B. Chaivanov, Hydrogen. Parameters of Combustion and Explosion. – M.:Fizmatlit (2008), 288 p.
3. J.E. Shepherd, Structural response to explosions. 1st European Summer school on hydrogen safety, The University of Olster, 2007
4. A. Teodorczyk, Mitigation of hydrogen-air detonations. 1st European Summer school on hydrogen safety, Belfast, 2006
5. J.H. Lee, Explosion hazards of hydrogen-air mixtures. 1st European Summer school on hydrogen safety, Belfast, 2006
6. A. Teodorczyk, Initiation of hydrogen detonation. 2nd European Summer school on hydrogen safety, Belfast, 2007
7. A. Teodorczyk, Limits of steady propagation of hydrogen deflagrations and detonations. 2nd European Summer school on hydrogen safety, Belfast, 2007
8. W. Breitung, Mechanistic safety analysis of hydrogen based energy systems. 2nd European Summer school on hydrogen safety, Belfast, 2007
9. (a) S.B. Dorofeev, Evaluation of safety distances related to unconfined hydrogen explosions Int. J. Hydrogen Energy **32**(13), 2118–2124 (2007). (b) S.B. Dorofeev, Evaluation of safety distances related to unconfined hydrogen explosions. International conference on hydrogen safety, Pisa, 2005
10. J.X. Wen, Hydrogen fires. 1st European Summer school on hydrogen safety, Belfast, 2006
11. P. Wolanski, Fourty years of investigation of diffusion ignition. Paper at the 7th international symposium on hazards, prevention and mitigation of industrial explosions, St. Petersburgh, 2008
12. (a) J.G. Quintiere, Fundamentals of premixed flames. 1st European Summer school on hydrogen safety, Belfast, 2006. (b) J.G. Quintiere, Fire plumes and jets. 1st European Summer school on hydrogen safety, Belfast, 2006

13. J.H.S. Lee, *The Detonation Phenomenon* (Cambridge University Press, 2008), 390 p.
14. J.E. Shepherd, Detonation in gases. PCI **32** (2008)
15. J.E. Shepherd, Deflagration to detonation transition loads. Proceedings of PVP-IS-PVT211, 2006. ASME pressure vessels and piping conference
16. B.E. Gelfand, M.V. Silnikov, *Barothermic Effect of Explosions* (Asterion, St. Petersburg, 2006), 658 p.
17. B.E. Gelfand, M.V. Silnikov, *Gaseous Explosions* (Asterion, St. Petersburg, 2007), 240 p.
18. B.E. Gelfand, M.V. Silnikov, *Volumetric Explosions* (Asterion, St. Petersburg, 2008), 374 p.

Abbreviations and Designations

a, b	Transverse and longitudinal dimension of detonation cell
BR	Blockage ratio
$C(t)$	Change of concentration with time
C	Fuel excess ratio
C–J	Chapman–Jouguet condition
c_0	Sound speed in fresh mixture
c_1	Sound speed in explosion products
D	Detonation velocity
D_i	Diffusion coefficient of *ith* component of mixture
Da	The Damköhler number
d	Tube diameter
d^*	Critical tube diameter for detonation propagation
d^{**}	Critical diameter for detonation propagation from a narrow channel to a wider tube
d_{f}	Critical diameter of a free cylindrical charge for detonation propagation
d_{r}	Igniter diameter
d_{cr}	Critical tube diameter for flame quenching
d_{II}	Critical gap for flame quenching
DDT	Deflagration-to-detonation transition
E	Igniter energy, energy of initiation
E_{min}	Minimum igniter energy, minimum energy of initiation
$E*$	Critical energy of spherical detonation initiation
EC	Explosion chamber
FA	Flame acceleration
FAM	Fuel+air mixtures
Fr	Froude number
h	Height of diffusion flame over a burner rim
HAM	Hydrogen + air mixtures
HCOM	Hydrogen + carbon oxide mixtures
HCM	Hydrogen + hydrocarbon mixtures
HE	High explosive

HM	Hydrogenous mixtures
HOM	Hydrogen + oxygen mixtures
HRJE	Hybrid ramjet engine
I_+, I_-	Impulse of compression phase (+) and rarefaction (−) phases in an air blast wave
J	Fuel mass in a mixture
K	Karlovitz stretch-factor
K_{ext}	Stretch factor for flame quenching
Ka	Karlovitz number
K_p	TNT pressure equivalent of a gas explosion
K_I	TNT impulse equivalent of a gas explosion
K_f	Decrement of pressure attenuation behind a wave front
k	Proportionality factor
L	Tube length
L_f	Diffusion flame body length
L_{M}	Markstein length (scale)
L_d	Pre-detonation zone length
L_m	Minimum distance for transition to detonation
Le	Lewis number
ℓ	Turbulence scale
$\text{M}_1 > 1$	Detonation wave Mach number
$\text{M}_2 < 1$	Deflagration wave Mach number
Ma	Markstein number
n	Fan speed
n_u	Mole number of unburned mixture
n_b	Mole number of reaction products
n_{H2}	Hydrogen mole number
NPP	Nuclear power plant
NTP	Normal temperature and pressure conditions
P_0	Mixture initial pressure
P_1	Maximum pressure in incident detonation wave
P_2, $P_{\text{C–J}}$	Chapman–Jouguet point pressure
P_3	Maximum pressure at detonation wave reflection
P_{c}	Explosion products pressure
P_{cv}, P_{AICC}	Explosion pressure at constant volume combustion
P_{v}	Saturated water vapor pressure
P_{f}	Maximum pressure of compression wave
ΔP	Pressure difference
ΔP_{f}, ΔP_+	Maximum overpressure in compression wave
ΔP_-	Rarefaction wave amplitude
Pe	Peclet number
Q	Heat of combustion
q	Volume density of gas mixture energy
R	Universal gas constant

Re	Reynolds number
R_0	Tank radius, fuel-air mixture cloud radius
R_f, r_f	Flame front radius
RJE	Ramjet engine
RW	Rarefaction wave
S_u	Laminar flame velocity (combustion velocity)
${S_u}^0$	Planar flame velocity
S_b	Flame visible velocity
${S_u}^{\mathrm{st}}$	Laminar flame velocity in stoichiometric mixture
$S_u^{\max}$	Maximum velocity of laminar flame
S_{T}	Turbulent flame velocity (combustion velocity)
SW	Shock wave
T_0	Initial temperature of mixture
T_1	Combustion products temperature
T_2	Chapman–Jouguet point temperature
T_{si}	Temperature of self-ignition
T_3	Ignition temperature
T_b	Flame temperature
T_{ad}	Adiabatic flame temperature (adiabatic temperature)
t	Time
t^*	Retention interval in heated tank
Δt_{m}	Maximum blast pressure time
U	Combustion velocity in obstructed tube
U	Combustion wave velocity
U_{sp}	Spontaneous velocity of combustion front propagation
u'_Σ	Pulsation velocity
u'_x, u'_y, u'_z	Components of pulsation velocity along three coordinates
UCL LCL	Upper and lower concentration limits
V	Tank volume
W	Width of canal rectangular opening
X_{H2}	Hydrogen volume content in hydrogenous mixture
Y	Active additive concentration
Z	Volume content of inert diluent in mixture
Ze	Zeldovich number
α	Temperature index of flame velocity
β	Pressure index of flame velocity
α_{B}	Coefficient of excess air in hydrogenous mixture
ϕ	Equivalence ratio
φ	Droplets volume concentration
φ_0	Angle between transverse wave trajectory and generatrix
μ	Fraction of burned-out substance, molecular weight, fluid viscosity
$\pi = P_1/P_0$	Pressure rise level at combustion and in shock wave
ρ_0	Fresh mixture density
ρ_{bp}	Density of blast products

β_c	Volume concentration of fuel gas bubbles
γ_0	Specific heats ratio
γ_1	Specific heats ratio in combustion products
δ	Particle size of plug material
δ_0	Flame thickness
δ_L	Laminar flame thickness
δ_T	Turbulent flame thickness
Λ	Reduced distance
λ	Wave length
$\sigma = \rho_u/\rho_b$	Expansion ratio at combustion
τ_i	Self-ignition delay time
τ_+, τ_-	Duration of compression phase (+) and rarefaction phase (–) in air shock wave
Θ	Water weight concentration

Contents

Chapter 1
Fundamental Combustion Characteristics of Hydrogenous Mixtures

Keywords Combustion • Laminar flame • Turbulent flame

1.1 Laminar Flame Velocity

A laminar flame velocity is one of the fundamental characteristics of premixed combustible gas reactivity. It specifies an amount of mixture reacting across a unit flame front area per unit time. According to the classical definition, a laminar flame (combustion) velocity is the expansion rate of a flat one-dimensional flame front in the direction normal to the wave surface with respect to the unburned gas [1].

In the case of spherical flames, additional characteristics, such as the Karlovitz stretch factor [2] and the Markstein length [3, 4], are used to describe real curved flames.

1.2 Flame Stretch Rate (Stretch Effect)

Most real flames are subjected to local surface hydrodynamic deformation including the one that causes changing of the local curvature. It affects the velocity of the flame front propagation (further referred to as "flame velocity") and it is called a stretch or a stretch effect.

The Karlovitz stretch factor K denotes the rate of a flame front area change dA/dt with respect to the whole flame surface area [5]

$$K = \frac{1}{A}\frac{dA}{dt}.$$

The K factor has dimensionality s^{-1}, it can be expressed in terms of a flame front radius r_f for a spherical flame:

B.E. Gelfand et al., *Thermo-Gas Dynamics of Hydrogen Combustion and Explosion*, Shock Wave and High Pressure Phenomena,
DOI 10.1007/978-3-642-25352-2_1, © Springer-Verlag Berlin Heidelberg 2012

$$K = \frac{2}{r_f}\frac{dr_f}{dt}.$$

Here dr_f/dt is the flame velocity with respect to the burned gases and it is called a visible velocity S_b. The upper index “0“» is introduced for a stretch-free flat flame velocity $S_b{}^0$ in relation to the burned gases. The non-dimensional stretch, called the Karlovitz number, is found from the ratio:

$$\mathrm{Ka} = K \cdot \frac{\delta_0}{S_u^0},$$

where δ_0 – is the laminar flame thickness and $S_u{}^0$ – the flat (stretch-free) flame velocity.

Figure 1.1 demonstrates the flame velocity, $S_{u,}$ change in H_2 + air mixtures in relation to the Karlovitz number [6].

A flame initiated in the center of a premixed fuel + air volume continues to expand as a spherical cloud of combustion products and involves increasingly more volume of the unburned mixture. The stretch has maximum values at small flame radius r_f and gradually decreases when the spherical flame is expanding.

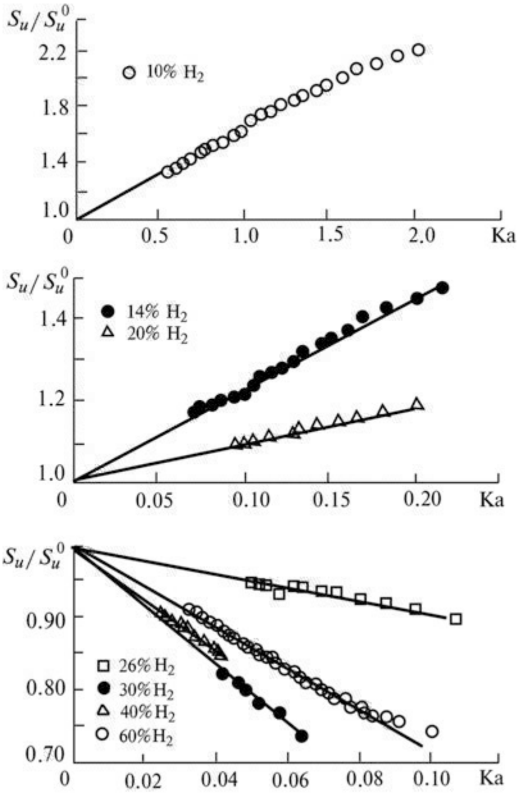

Fig. 1.1 The flame velocity change versus the Karlovitz number in H_2 + air mixtures at room temperature and 0.1 MPa pressure

In conformity with the curvature, for the divergent spherical flame, the stretch is positive, and for the convergent one – negative. For example, the negative stretch is observed near the tip of a flame stabilized in a Bunsen's burner. In general, the sign of the stretch is determined locally.

1.3 Markstein Length

Quantitative description of the stretch is a key problem for both laminar and turbulent combustion. Experimental data obtained for the stretch effect on a premixed flame have been proven by theory and by detailed computer simulation [7–14]. It has been found that when the stretch value is small, its effect on the flame velocity is linear. The change in the burning velocity can be expressed by the so called Markstein length [3, 4, 11, 12] found from the equation:

$$S_u = S_u{}^0 - L_M K.$$

The Markstein length – is a quantitative measure of the flame response to the stretch. Here S_u – curved flame velocity, $S_u{}^0$ – flat flame velocity, L_M – Markstein length, K – Karlovitz stretch factor.

The characteristic dimensional parameter L_M takes into account the flame curvature effect on the burning velocity. The higher its absolute value, the stronger the curvature effect is. The Markstein length relation to the laminar flame thickness $\delta = a/S_u$, where S_u – the laminar flame velocity, is known as the Markstein number $\mathrm{Ma} = L_M/\delta$. Table 1.1 [15] presents the Markstein length for hydrogen-air mixtures at 298 K and 0.1 MPa

Figure 1.2 illustrates the change in the Markstein length for H_2 + Air mixture in relation to the stoichiometric ratio value.

Table 1.1 The Markstein length for H_2 + air mixture

% H_2	10	15	20	29.6	40	50	60
L_M, mm	−0.350	−0.209	−0.104	0.021	0.062	0.091	0.178

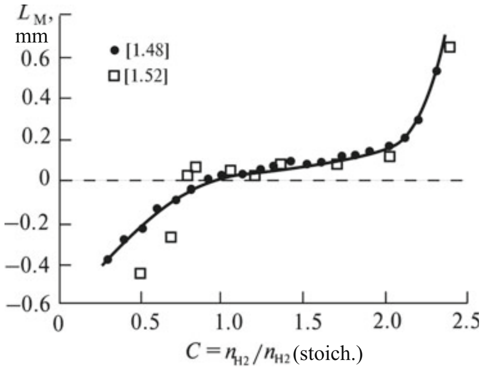

Fig. 1.2 The Markstein lengths found experimentally for spherically divergent flames in H_2 + air mixture at room temperature and atmospheric pressure [15, 50]

1.4 Lewis Number and Selective Diffusion

In general, the stretch has minimum effect on an adiabatic diffusion-neutral undistorted flame, but it can change by the selective diffusion phenomenon [7, 8].

Three types of diffusion are known in the flame: heat diffusion (thermal diffusivity) (a), limiting reagent diffusion (D_i) and excessive reagent diffusion (D_j). Having three diffusion factors and comparing D_i with a and D_i with D_j for non-stoichiometric and near stoichiometric mixtures, it is possible to obtain two criteria for a selective diffusion. These two criteria specify the non-unity Lewis number effect ($\mathrm{Le} = a/D_i$) and the differential diffusion effect (D_i/D_j).

The flame behavior and its temperature depend on the relative velocities of the heat and the mass diffusion. If $\mathrm{Le} = 1$, then the total enthalpy is conserved and the flame temperature T_b corresponds to the adiabatic temperature T_{ad}. If $\mathrm{Le} < 1$, then the flame temperature $T_b > T_{\mathrm{ad}}$. If $\mathrm{Le} > 1$, then $T_b < T_{\mathrm{ad}}$.

When the limiting reagent possesses the larger diffusion coefficient, its concentration in the reaction zone becomes close to stoichiometric, and this leads to a temperature rise and intensive burning. The opposite effect is observed when the limiting reagent is less diffusible.

The Lewis number $\mathrm{Le} = a/D$ is the mixture thermal diffusivity a ratio to the limiting reagent diffusion coefficient D. In lean mixtures the limiting reagent is hydrogen and in rich mixtures – oxygen.

The Lewis number specifies the relative significance of thermal diffusion and mass diffusion and is used as a criterion of the diffusion-thermal instability of a laminar flame. For a multi-component system the Lewis number of each component presented in Table 1.2 [16] can be calculated.

Table 1.2 The Lewis numbers of H_2 + air flame for three values of excess fuel factor ϕ

ϕ	$\mathrm{Le}_{\mathrm{H2}}$	$\mathrm{Le}_{\mathrm{O2}}$	Le_{O}	Le_{H}	$\mathrm{Le}_{\mathrm{OH}}$	$\mathrm{Le}_{\mathrm{H2O}}$	$\mathrm{Le}_{\mathrm{H2}}$	$\mathrm{Le}_{\mathrm{H2O2}}$	$\mathrm{Le}_{\mathrm{N2}}$
0.7	0.31	1.13	0.72	0.18	0.74	0.83	1.12	1.13	1.19
1.0	0.33	1.20	0.78	0.20	0.79	0.88	1.20	1.21	1.35
1.4	0.37	1.36	0.89	0.23	0.91	1.02	1.36	1.37	1.63

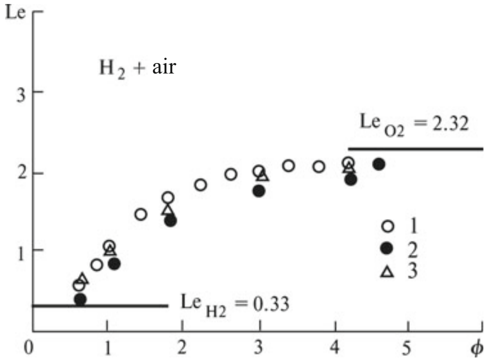

Fig. 1.3 The Lewis numbers found experimentally for the velocities of spherical divergent flames – *1*, spherical convergent flames – *2*, and head-on streams of stationary flames – *3*, in H_2 + air mixtures at room temperature and atmospheric pressure [16]

Figure 1.3 presents reliable experimental data on the Lewis numbers depending on the excess fuel factor ϕ for H_2 + air mixtures. Those data have been obtained for spherically divergent and spherically convergent flames, and for flames stabilized by opposed jet configurations.

1.5 Diffusion-Thermal and Hydrodynamic Flame Instability

The flame stretch-effect influences a laminar flame velocity due to the thermal and mass selective diffusion [7–12]. This effect may cause a flame front instability depending on the sign of the Markstein length. When a Markstein length is negative, the flame laminar velocity increases with the stretch growth.

The flame front concavity (bulging) with respect to the combustion products possess a positive (negative) stretch, and their growth makes the flame unstable. At a positive Markstein length, the flame laminar velocity falls with the stretch increase and the flame surface curvatures reduce, which indicates flame stability.

Those effects may include a selective mass diffusion with respect to the thermal diffusion, which leads to a diffusion-thermal (DT) instability [1, 8, 17, 18]. A selective diffusion of one reactant with respect to another, results in diffusion-diffusion (DD) [8] or both types of instability.

At a neutral and stable selective diffusion and a slight buoyancy force impact, the laminar flames demonstrate hydrodynamic instability.

Landau and Darrieus pioneering works on hydrodynamic instability of a flat laminar flame are well known [1]. According to Darrieus-Landau theory, small perturbations, independent of the wave length, make a flat flame unstable.

Virtually, there exist mechanisms leading to the stable propagation of a flame, if the Reynolds numbers are not too large. A mechanism of hydrodynamic stability consists of acceleration of denser reactants towards the reaction products of lower density. Markstein has analyzed [3, 4] this mechanism in a flat flame, he considered the flame surface as a density discontinuity.

The problem of spherical flame stability was studied by Istratov and Librovich [19] and has been intensively developed [20–26]. It was found that the perturbation progressing on large–scale spherical flame surfaces results in surface turbulence generation [27–29]. This phenomenon can be described by fractal mechanisms [30–33].

The instability caused by HD and DD phenomena is often observed in lab-scale experiments with hydrogen + air mixtures. Photographs of a spherical flame in mixtures containing 10% and 50% hydrogen [2, 34] denote a smooth combustion front in the rich mixture and a cellular front in the lean mixture. In closed combustion chambers the perturbation of the flame front increases due to the impact of pressure waves reflected from the walls [35, 36]. In quick-burning mixtures a “hedgehog”-like structure of the front appears when the flame approaches the walls.

The increase in the burn velocity, when a spherical flame becomes curved, cellular and turbulent, is explained by the growth of the flame surface. A lot of experimental and theoretical investigations have been devoted to the propagation of curved and cellular flames [7–14, 17–39].

In the above mentioned investigations special attention is given to the spherical flame. In experiments with a spherical curved flame, the radius can be specified as the radius of a smooth sphere with a volume equal to that of the burned gas. The amount of curvature can be found from the ratio of total surface of the curved flame to the smooth sphere surface. A similar method is used for investigation of turbulent combustion of quasi-spherical flame sources.

1.6 Turbulent Flame Velocity

Turbulent flame velocity S_T – is a frequently measured parameter for turbulent combustion of premixed gases. It reflects the complex interaction of the combustion chemistry and turbulence. The non-dimensional correlations binding this parameter to the other key characteristics have been derived based on asymptotic analysis.

In particular, Bradley and co-authors [40–45] have collected more than 1,600 experimental data sets on S_T, normalized to the laminar burning velocity $S_u{}^0$. The data interrelate $S_T/S_u{}^0$ with the curvature factor that includes the effective mean-square normalized pulsation velocity $u'/S_u{}^0$ in cold premixed gases and the Karlovitz factor K multiplied by the Lewis number Le. The diagrammatic presentation of the aforementioned data shows the $\mathrm{Re}/\mathrm{Le}^2$ parameter effect, where Re is the turbulent Reynolds number. These experimental data are the source for verification of turbulent combustion models including a laminar flamelet approach [46, 47].

The Borghi diagram (Fig. 1.4) presents feasible turbulent combustion regimes [48]. The diagram shows the ratio L_T/δ_L (L_T – the Lagrangian integrated turbulent scale, δ_L, – the laminar flame thickness) plotted against the ratio $u'/S_u{}^0$ (u' -the pulsation velocity, $S_u{}^0$ – the laminar burning velocity). The lower left corner of the diagram presents the laminar regimes of combustion. The line on which the turbulent Reynolds number $\mathrm{Re}_T = 1$ is the boundary between the laminar and

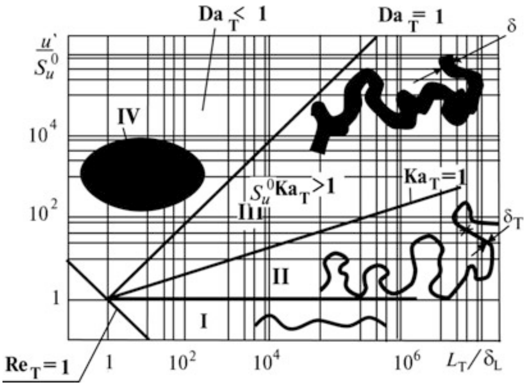

Fig. 1.4 The Borghi diagram for definition of turbulent combustion regimes [48]

turbulent combustion regimes. Special characteristics of turbulent flames depend on the Karlovitz $\mathrm{Ka_T}$ and the Damkohler $\mathrm{Da_T}$ turbulence numbers.

In the region I, where the pulsation velocity does not exceed the laminar flame velocity, the turbulent flame possesses a curved front of thickness similar to that of the laminar front. With the pulsation velocity growth, the level of curvature increases and the flame can lose its continuity.

However, in region II, which boundary corresponds to the Karlovitz turbulence number $\mathrm{Ka_T} = 1$, the reaction zone thickness is equal to that of region I. It means that the chemical reaction is completed within t_c, a negligibly small value in comparison with the characteristic time of the turbulent mixing t_T. The t_T/t_c ratio is called the Damkohler number $\mathrm{Da_T}$.

In region III, bounded by the lines corresponding to $\mathrm{Ka_T} = 1$ at the bottom and $\mathrm{Da_T} = 1$ at the top, the reaction zone thickness grows and the flame cannot be described by the flamelet approach based on the laminar curved flame model. As a limiting case the “ideal mixing reactor” model (the chemical reaction speed is neglected in comparison with the turbulent mixing time) is considered.

At comparable turbulent scale and reaction zone thickness, the combustion in region IV occurs in a volumetric manner similar to a thermal explosion.

1.7 Mixture Composition

In the literature the mixture composition can be specified in different ways.

Usually, for this purpose, a fuel volume content (%) is used and an equivalence ratio is defined by the following formula

$$\phi = \frac{fuel/oxydizer}{(fuel/oxydizer)_{stoich.}},$$

The oxidizer in this ratio is pure oxygen O_2 or oxygen/nitrogen mixture (O_2 + 3.76 N_2) close to the air composition.

If the fuel is hydrogen and the oxidizer is air the following equation can be applied:

$$\phi = \frac{\%\,\mathrm{H_2}/(100\% - \%\,\mathrm{H_2})}{0.42}.$$

The numerical factor 0.42 corresponds to the stoichiometric content of hydrogen in air (29.6% volume). With respect to the fuel, mixtures with $\phi < 1$ are called lean and with $\phi > 1$ – rich ones.

Sometimes, a value called the fuel excess ratio is used:

$$C = \frac{n_{\mathrm{H}_2}}{(n_{\mathrm{H}_2})_{stoich.}},$$

where n_{H_2} – hydrogen mole number in the mixture, and $(n_{\mathrm{H}_2})_{stoich.}$ – hydrogen mole number at the stoichiometric H_2/O_2 ratio.

For multi-component mixtures containing several types of fuels and additives the percentage of each component is specified. The condensed components are usually specified as mass fractions.

1.8 Macroscopic Combustion Parameters of Hydrogenous Mixtures

The effects of hydrogenous mixture combustion in a closed space have been described by a number of macroscopic physicochemical values that will be useful for our further description. We restrict our attention to such values for hydrogen-oxygen (HOM) and hydrogen – air (HAM) mixtures.

Figure 1.5 presents the explosion pressure (P_c)/hydrogen volume fraction diagrams of the explosion of a combustible mixture (initial pressure $P_o = 0.1$ MPa and temperature $T = 293$ K) occurring as a result of hydrogen combustion in oxygen (1) or in air (2). The diagrams are based on experimental results [49] measured for a 6-L vessel.

Each case of explosion is characterized by its own rate of pressure rise dP/dt. Sometimes this parameter is applied to define the level of explosive risk according to the factor $K = V^{0,33}$ [dP/dt]. Here V is the volume of the explosion chamber. Figure 1.6 presents the rate of the pressure rise as a function of hydrogen-air mixture composition at different conditions.

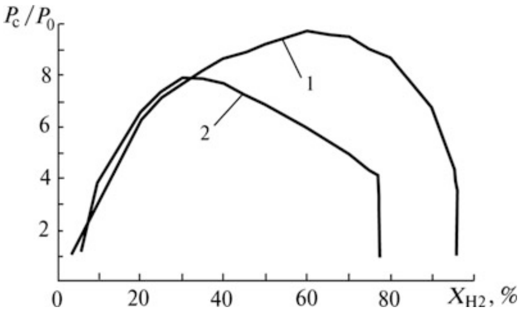

Fig. 1.5 The pressure-hydrogen volume fraction diagrams for hydrogen-oxygen (*1*) and hydrogen-air explosions (*2*) of a combustible mixture at $P_o = 0.1$ MPa and $T = 293$ K [49]